Pergamon

Int. J. Multiphase Flow Vol. 24, No. 2, pp. 213–223, 1998

Printed in Great Britain
PII: S0301-9322(97)00049-9
0301-9322/98 $19.00 + 0.00

TURBULENT FLUID AND PARTICLE INTERACTION IN THE BOUNDARY LAYER FOR CROSS FLOW OVER A TUBE

J. R. FAN, X. Y. ZHANG, J. JIN, Y. Q. ZHENG and K. F. CEN
Department of Energy Engineering, Zhejiang University, Hangzhou 310027, People's Republic of China

(Received 1 January 1997; in revised form 1 July 1997)

Abstract—The influence of solid particles on the flow characteristics of the boundary layer for cross flow over a tube has been experimentally studied. A phase-Doppler anemometer was used to measure the mean and fluctuation velocities of both phases. Two separate tests were conducted with two particle size ranges (30–60 μm and 80–150 μm) and the freestream velocity and solid mass loading ratio were fixed, allowing the effects of particle sizes on the shape of the mean velocity profile and on the turbulent intensity levels. The measurements clearly demonstrated that the larger particles damped fluid turbulence. For the smaller particles, this damping effect was less noticeable. The measurements further showed a delay in the separation point for two phase turbulent cross flow over a tube. © 1998 Elsevier Science Ltd. All rights reserved

Key Words: particle and fluid turbulence interaction, two-phase cross flow over a tube, boundary layer, PDA measurement

1. INTRODUCTION

Particle-laden cross flow over tubes occurs in many engineering situations, such as solid fuel combustion systems associated with fluidized bed reactors, shell-and-tube heat exchangers, aerosol sampling and air cleaning. However, only a few studies of two-phase cross flow over tubes have been reported in the literature.

Although most gas–solid systems encountered in practice are turbulent, the case of laminar boundary-layer motion of a gas–solid suspension over a flat plate was treated by Soo (1965, 1966) to develop some basic understanding, via mathematical procedures, of interaction of a gas–solid suspension with a boundary. The simplest non-trivial case of two-dimensional motion of a gas–solid suspension over a flat plate consists of an incompressible gas phase with uniform solid concentration of particles of one size in the freestream only. Soo noted that the fluid phase stream function ψ can be determined by well known methods such as the Howarth transformation (Howarth 1936) with the motion of the particle phase determined with $f(\eta) \propto \psi/x^{1/2}$, where f is the well known Blasius function, $\eta = y(U_0/vx)^{0.5}$, with U_0 the freestream velocity, x and y the distances along and normal to the flat plate, and v the kinematic viscosity. A separate set of ψ_p for the particle phase can be determined from the solution (Soo 1965). A similar study of flow of a suspension over a flat plate was made by Marble (1963) and Singleton (1965). These studies were done for the same reason to develop basic understanding; laminar boundary-layer motion of a gas–solid suspension was studied in spite of the fact that almost all flow machineries involve turbulent flow.

Grass (1974) recorded the details of the suspension process in a turbulent boundary layer on a flat plate. It was observed that sand particles were carried up from the wall region through virtually the total boundary layer thickness. Some measurements on the larger particle (3.0 mm) motion near a wall were made by Sumer and Deigaard (1981) using a photogrammetric system. It was noted that, with a smooth bottom wall, the measured kinematic quantities characterizing the particle motion were in accordance with available information on the bursting phenomena. They suggested that this was perhaps a mechanism to cause particle suspension in the flow.

Inoue *et al.* (1986) measured the flow characteristics around a cylinder of two-phase (air–water) cross flow in Reynolds number range 5000–80,000. They found that high void fraction regions, with the local void fraction about three to four times higher than the freestream value, were produced near the separation point. As the mean velocity in the main flow increased, this peak void fraction also increased and the location of the peak void fraction came closer to the cylinder. However, they did not measure void fraction upstream of the tube. From the observation of the flow patterns, they noted a liquid-rich layer in the front and in the rear of the tube. The liquid layer became thicker in the front of the cylinder, and became thinner in the rear of the cylinder when the mean velocity increased.

In the second part of the same study, Yokosawa *et al.* (1986) measured the drag on a single tube under two-phase cross flow in the Reynolds number range 4000–300,000 and for low void fractions (0–0.1). They found that the drag coefficient decreased with increasing void fraction for two-phase Reynolds numbers sufficiently below the single-phase critical Reynolds number. But for Reynolds numbers above the critical value, the drag coefficient was found to gradually increase with increasing void fraction. A recent work by Joo and Dhir (1994) has measured the drag on a single tube and on a tube in an array under two-phase cross flow. They found also two-phase drag coefficients were much higher than those for single-phase flow. The ratio of two-phase to single-phase drag coefficients decreased as the Reynolds number became larger or the inertia of the base flow increased.

Rashidi *et al.* (1990) studied the particle–turbulence interaction in wall turbulent flows. A series of experiments varying particle size, particle density, particle loading and flow Reynolds number Re has been conducted. They found that the larger polystyrene particles (1100 μm) caused an increase in the number of wall ejections, giving rise to an increase in the turbulent intensities and Reynolds stresses, while the smaller polystyrene particles (120 μm) brought about a decrease in the number of wall ejections, causing a decrease in the turbulent intensities and Reynolds stresses. Based on their observations, it appears that particle transport is controlled mainly by the ejections originating from the liftup and breakdown of the low-speed streaks in the wall regions.

The effect of small particles on fluid turbulence in a flat-plate, turbulent boundary layer in air has been investigated by Rogers and Eaton (1991). Their measurements clearly demonstrated that the particles suppressed fluid turbulence, and showed a strong correlation between the degree of turbulence suppression and the particle concentration in the log region of the boundary layer. They attributed the turbulence suppression to an increase in the dissipation. The power spectra showed that for the normal fluctuations the power spectrum shifts to higher frequencies relative to the streamwise fluctuations, therefore implying that particles did not closely follow the fluid fluctuations in the normal direction. However, they were unable to clarify their results in light of the observed dominant flow events near the wall.

In addition to turbulence effects, changes in boundary layer profiles have been measured by Lee and Durst (1982) and by Murray (1989) for gas–particle suspension flows in pipes and across a staggered tube array respectively. For both of these, reductions in the boundary layer physical thickness were observed with higher velocity gradients at the wall so that higher local heat transfer coefficients would be expected (Murray and Fitzpatrick 1991). Fitzpatrick *et al.* (1992) also studied the effects of particles on the boundary layer characteristics in the near separation of a gas–particle cross flow.

However, it should be pointed out that until very recently it was impossible to find in the literature a well-documented experimental study of the particle and fluid turbulence interaction in a boundary layer for cross flow over a tube. Generally, gas–particle turbulence interaction, such as small particles attenuating turbulence and large particles augmenting it, has also been assessed on the basis of the ratio of the relative particle to eddy size by Gore and Crowe (1989) and in terms of the particle Reynolds number by Hetsroni (1989). The crossover between attenuation and amplification was well correlated by both of these parameters, but the level of attenuation was widely scattered. Much of the scatter is due to poor control of experimental conditions and to difficulties in measuring gas phase velocity in the presence of a high concentration of particles. The turbulence intensity may be affected by the flow Reynolds number, the

class of flow (e.g. homogeneous, wall-bounded, or free shear flow), the particle diameter, the density ratio between fluid and particles, and the mass loading ratio.

The present paper reports the results from an experimental study aimed at assessing the particle and fluid turbulence interaction in the boundary layer for cross flow over a tube, especially in the near separation region. The measurements made in the near separation region will indicate significant unsteadiness associated with the movement of the separated shear layer. Experiments have been conducted for two separate cases with two particle size ranges (30–60 μm and 80–150 μm) and the fixed freestream velocity and solid mass loading ratio. The objective is to better understand the influence of the particles on the boundary layer characteristics for a tube in cross flow. A phase-Doppler anemometer (PDA) was used to measure the mean and fluctuating velocity distributions of the gas and particle phase. Both mean and fluctuating velocity in the boundary layer region at 95° to 110° from the front stagnation point were obtained. The data resulting from the present study can be used to enhance the understanding of two-phase cross flow over the tubes, to evaluate the effects of the present particles on the characteristics of the boundary layer, and to provide a useful basis for validating proposed models for the two-phase boundary layer.

2. EXPERIMENTAL SETUP

2.1. *Test facility*

The test facility for the particle-laden boundary layer of cross flow over a tube is shown schematically in figure 1. The test facility mainly comprised an exhaust blower, a cyclone, and a tunnel that includes the particle feeding section, the diffusion section and the test section. At the beginning of the tunnel is a contraction, which is used to reduce the entrance disturbance of the air flow, thereby making a shorter length of the diffusion section necessary. Air was drawn into the tunnel and was contaminated with flow tracer (titanium-oxide power). The flow then passed through a 2 m long diffusion section. Particles were fed in at the beginning of the diffusion section, and downstream of the particle feeder a set of grids was mounted to enhance particle/fluid flow mixing. Before entering the test section, the particle-laden flow passed through a 3:1 contraction and a section of honeycomb which was mounted at the entrance of the test section. The

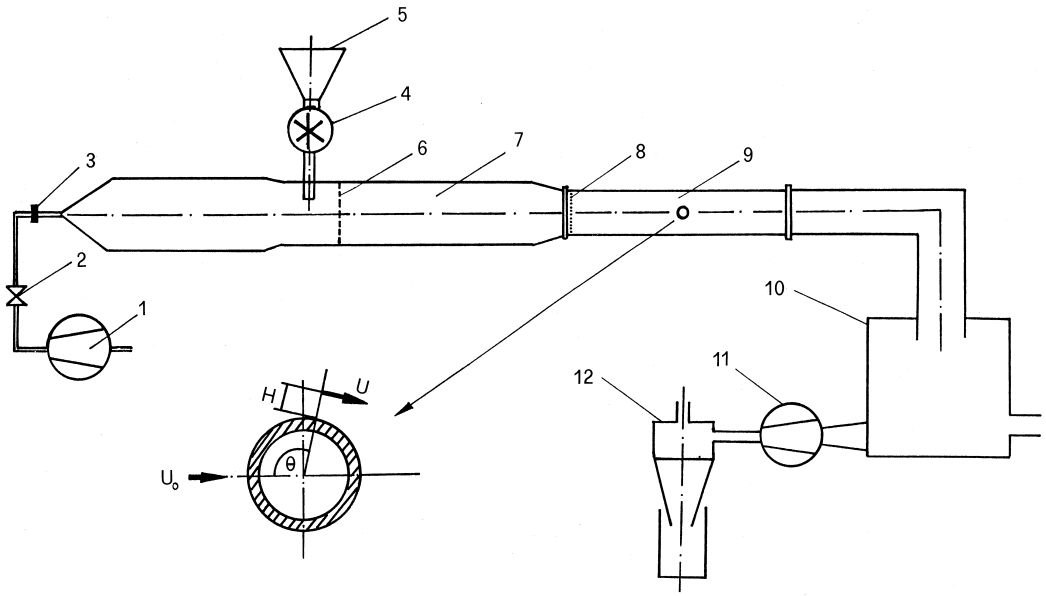

Figure 1. Schematic diagram of the experimental facility (1, blower; 2, throttle valve; 3, orifice flowmeter; 4, particle feeder; 5, particle reservoir; 6, grid set; 7, diffusion section; 8, honeycomb; 9, test section; 10, stagnation chamber with bypass; 11, exhaust blower; 12, cyclone separator and filter system).

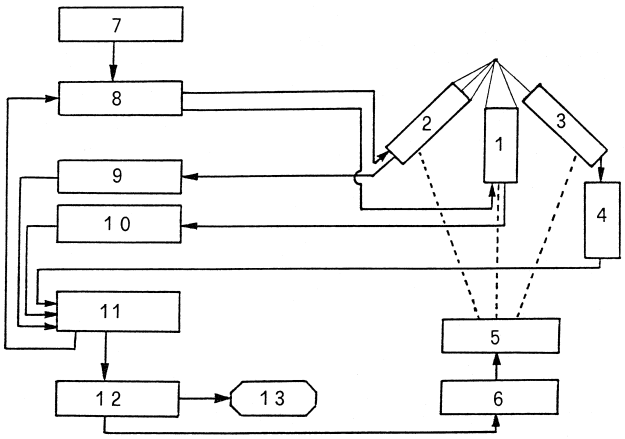

Figure 2. Schematic diagram of PDA system (1, 1D transmitter; 2, 2D transmitter; 3, receiver; 4, beam expander; 5, 3D traverser; 6, traverser communicator; 7, laser (Ar^+-ion); 8, Bragg cell; 9, blue beam expander; 10, violet beam expander; 11, date processor; 12, PC; 13, data output).

use of the contraction and the honeycomb additionally ensured a fairly uniform distribution of the particles in the cross-section at the entrance of the test section.

The test section was a 20 cm wide, 20 cm high and 100 cm long rectangular duct, at the center of which a glass tube with a diameter of 36 mm was horizontally fixed in the spanwise (z) direction. The boundary layer was developed when air and particles flowed over the tube. In order to allow optical access, all the test section walls were made from optical glass. These walls and the glass tube may be regarded as very smooth. Such a smooth surface facilitates elimination of the influence of the wall roughness on the particle-laden boundary layer flow.

At the end of the tunnel, particles were separated from the air using a cyclone separator and then the air flowed into an exhaust blower.

2.2. *PDA system and signal processing*

A three-component PDA was used for the present study. This instrument simultaneously measures velocities of the gas and particle phases. Figure 2 shows the PDA optics together with the data processing system. The PDA optics were mounted on a three-dimensional traversing system with stepper motors, which allowed a computer controlled traversing with a minimum traverse of 12.5 μm. A continuous power-adjustable argon-ion laser with a maximum light power of 5 W was used for a light source. The PDA transmitting optics were one based on 60X Fiber Flow, in which a built-in Bragg cell was used for frequency shifting. The transmitters split the incident beam into six of three colors, green, blue and violet, respectively. The two green beams were transmitted by a one-dimensional transmitter and the other four were transmitted by a two-dimensional transmitter. For the present measurement, the x-component of the velocity was measured with the green beams and the y-component was obtained with the blue and the violet. With the configuration used here, the measuring volumes had the dimensions of 0.16 mm $\times$ 0.16 mm $\times$ 0.5 mm with the largest dimension along a direction parallel to the z-wise direction.

The receiving optics were a 57×10 PDA. The scattered light from particles was collected by the receiving optics and then transformed into electrical signals by photomultipliers. The photomultipliers were specially designed for a wide range of linearity between light intensity and electrical output signal. The electrical signals, when bandpass filtered and amplified, were transferred to a processor which was connected to the photomultipliers.

The signal processing was based on a covariance processor (type 58n50 PDA enhanced signal processor) and a typical 486 personal computer. This processor implemented the covariance function of two Doppler signals for phase and frequency detection. A burst detector based on a three-level detection scheme was used to produce the trigger signal to initiate the data acquisition for measurements of phase and frequency. By implementation of the covariance function

and this scheme, the sensitivity of the processor to signal noise was reduced to such a low level that high reliability and accuracy might be achieved even for low SNR.

The output of the processor was transferred to a PC, which was connected to the processor by an interface. This computer was used to control the signal and receive the data from it for interpretation and post-processing. A special high speed direct access memory (DAM) method allowing a transferring rate with the maximum limit of 170,000 bytes/s was used for data transfer between the processor and the computer to give the system the capability to handle data rates in excess of 10,000 particles per second, which is much higher than needed for the present measurement. The accuracy of this apparatus at system level was 4% for size measurement and 1% for velocity measurement.

3. EXPERIMENT RESULTS

In the present study, we aimed at accessing the interactions between the turbulent fluid and the particle. Titanium oxide powder (0–10 μm) was used as flow tracer. The particles used for the particle phase had a material density (ρ_p) of 2650 kg/m^3. Microscopic examination showed that most of the particles were merely spherical. Two different size ranges, 30–60 μm and 80–150 μm, with mean diameters (d_p) of 40 μm and 120 μm respectively were used. Two separate experiments were carried out for the two size ranges at the same mass loading ratio of 0.25 and for the unladen (air) flow with all other conditions unchanged. Considering the symmetry of the geometry, boundary-layer profiles of both mean and fluctuating velocity were measured for the symmetrical section at $\theta = 95^\circ$ to 110° from the front stagnation point. At each measurement point 20,000 samples were collected. The freestream velocity and the freestream turbulence intensity at the test section were 14.4 m/s and 3% obtained for the unladen case by a PDA measurement.

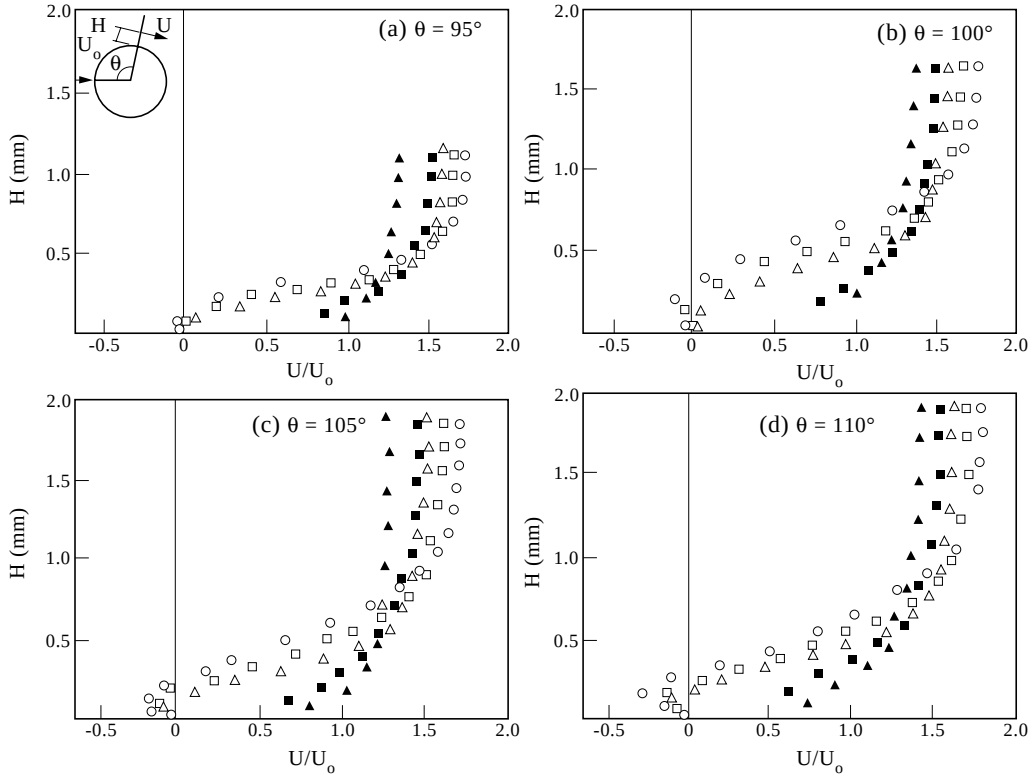

Figure 3. Mean tangential velocity profiles in the boundary layer (○, single-phase flow; □, two-phase flow, $d_p = 40$ μm; △, two-phase flow, $d_p = 120$ μm; open symbols, gas phase; closed symbols, particles). (a) 95°; (b) 100°; (c) 105°; (d) 110°.

3.1. *Measurements in the mean velocity profiles*

The mean tangential velocity (U) profiles measured in the boundary layer for the single-phase (air) flow and two particle-laden flow cases are shown in figure 3, where the results are normalized by the freestream velocity U_0. It is seen from figure 3 that both gas and particle phases are accelerated to attain tangential velocities in excess of the freestream velocity U_0, however the particles lag behind the gas owing to their inertia in the outer region, where the flow characteristics approach those of the mainstream flow. As seen from this figure, in the outer region the larger particles of 120 μm move at slower mean velocities than the fluid velocities. Namely, as the particle diameter increases the relative particle–fluid velocity also increases. Due to their higher inertia, the larger particles ($d_p = 120$ μm) exhibit even lower velocities than the smaller particles ($d_p = 40$ μm). On the contrary, particles of both sizes have higher tangential velocities than the gas phase in the middle region, where a large velocity gradient exists.

The comparison of the gas phase velocity profiles of the single-phase flow and particle-laden flow shows that there exists a minor decrease in mean velocities for the particle-laden flow case with the larger particles in the outer region, but an increase is observed distinctly in the middle region, especially at 100° to 105°. However, this modification is less noticeable for the smaller particles. This change leads to a considerable reduction in the physical thickness of the boundary layer in particle-laden flow cases. It indicates that a mass loading ratio of particles as great as 0.25 may cause some modification of the mean fluid velocity. This distinct modification is thought to arise from the momentum transfer between the gas and the particle phase, which will be discussed in detail in Section 4. A careful examination of figure 3(a) finds that the boundary layer has separated from the wall at $\theta = 95°$ for the single-phase flow, while the presence of the particles ($d_p = 40$ μm) has caused a definite delay in boundary layer separation with flow stagnation at the wall moving from 95° to 100°. For the particle-laden flow with larger particles ($d_p = 120$ μm), the delay of the boundary layer separation is observed to be greater. The point of

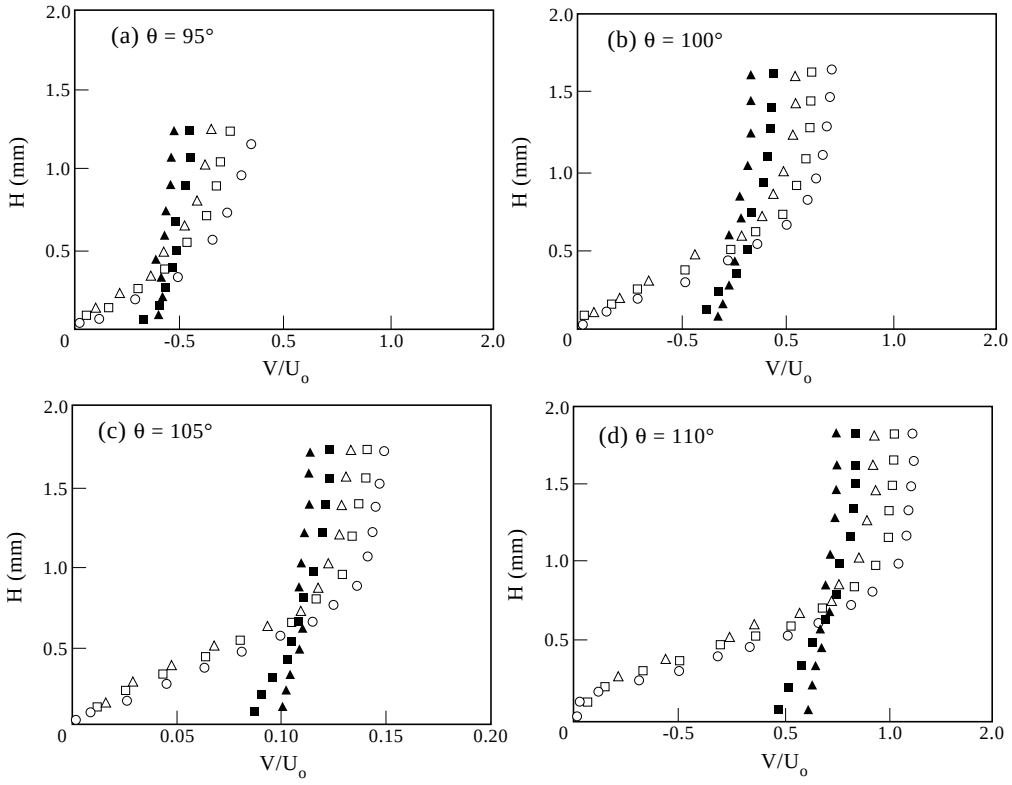

Figure 4. Mean radial velocity profiles in the boundary layer (○, single-phase flow; □, two-phase flow, $d_p = 40$ μm; △, two-phase flow, $d_p = 120$ μm; open symbols, gas phase; closed symbols, particles). (a) 95°; (b) 100°; (c) 105°; (d) 110°.

separation has now shifted to $\theta = 105^\circ$. Similarly, the momentum transfer from the particles to the air flow in the boundary layer regions close to the wall has contributed to this delay.

The distributions of the non-dimensional mean radial velocities, V/U_0, of the gas and particle phases for the three cases are demonstrated in figure 4. Similarly, the particles show lower mean radial velocities than the gas phase in the outer region of the boundary layer. In the middle and near wall region, the gas phase velocity is restricted in the radial direction by the wall and the particles exhibit comparatively higher velocities. This result is probably a reflection of the particle inertia and the particle/wall interaction. Actually, the velocity differences between the two phases (gas and particles) in the radial direction are small compared with those in the tangential direction.

3.2. *Measurement in the r.m.s. velocity profiles*

The measured r.m.s. velocity profiles of the gas and the particle phase are shown in figure 5 for the tangential component $\sqrt{\overline{u'^2}}$ and in figure 6 for the radial component $\sqrt{\overline{v'^2}}$, where the results are also made non-dimensional by the freestream velocity U_0. For comparison, we plot the profiles of the r.m.s. velocities for the single-phase (air) flow together with those for the two separate particle-laden flow cases in the same figure. Although the r.m.s. velocity profiles for the particle-laden flow are similar to those for the single-phase flow, some reduction of mainstream r.m.s. levels has been measured for the gas–particle cases. The turbulence intensity of the gas phase is consistently reduced by the presence of the particles in the near wall region. Within the boundary layer, the turbulence of the gas phase for the particle-laden flow cases is attenuated by 5% to 15%. This result falls also into particle induced fluid turbulence attenuation which was previously documented by Tsuji *et al.* (1984) and Rogers and Eaton (1991).

It is seen from figure 5 that there exists a peak located near the wall in the r.m.s. velocity profiles of the gas phase for both the single-phase flow and the particle-laden flow cases. The maxi-

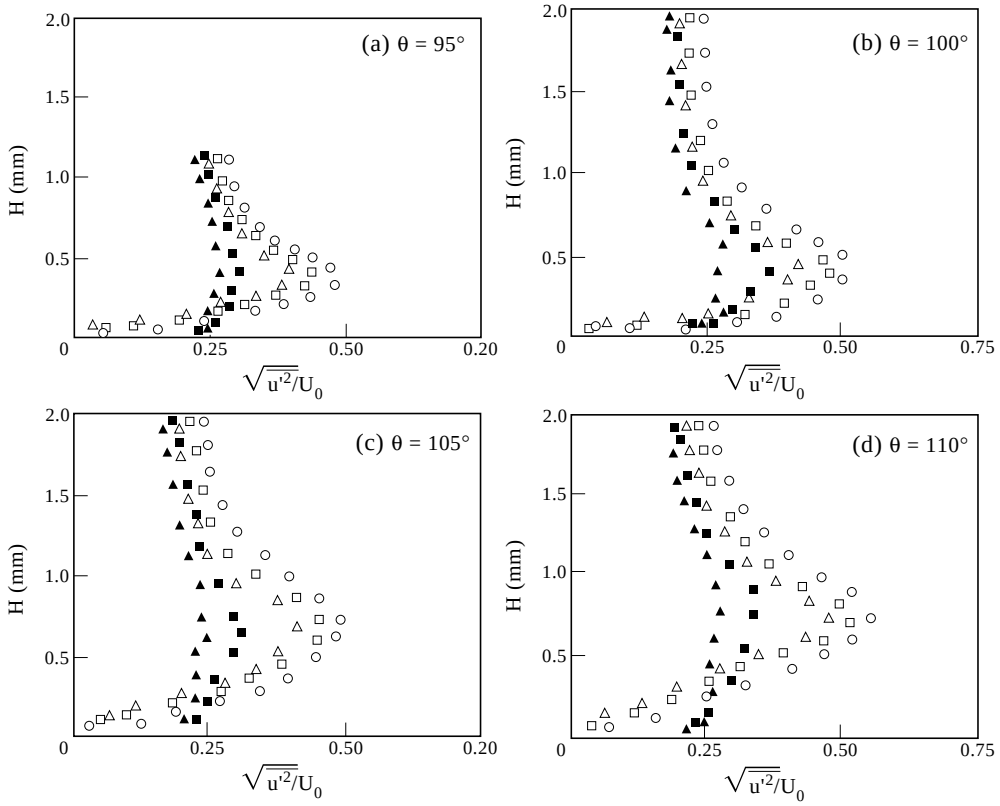

Figure 5. Tangential r.m.s. velocity profiles in the boundary layer (○, single-phase flow; □, two-phase flow, $d_p = 40\ \mu$m; △, two-phase flow, $d_p = 120\ \mu$m; open symbols, gas phase; closed symbols, particles). (a) 95°; (b) 100°; (c) 105°; (d) 110°.

mum value becomes greater accompanied by a farther location of the peak from the wall at an increasing angle from the front stagnation point, θ.

On the other hand, the tangential particle velocity fluctuations are generally lower than the corresponding fluid turbulent velocity fluctuations of the gas phase for both the 40 μm and 120 μm diameter particles. Note that the smaller particles ($d_p = 40$ μm) with shorter Stokes time constant respond more readily to the fluid velocity fluctuations, they have higher r.m.s. velocities than the larger ones ($d_p = 120$ μm). The radial velocity fluctuations of the particle phase are lower than those of the fluid with an exception only in the near wall region. This exception may be physically plausible since the fluid turbulence intensity is considerably suppressed in the normal to the wall direction, but the particles only slowly respond to the decrease in the fluid turbulence velocity fluctuations of the gas phase.

Figure 7 demonstrates the distribution of the normalized turbulent shear stress of the gas phase, $\overline{u'v'}/U_0^2$, and the measured values of the quantity for the particle phase. The distributions of $\overline{u'v'}/U_0^2$ show the same trend as those of the velocity fluctuations, $\sqrt{\overline{u'^2}}$ and $\sqrt{\overline{v'^2}}$, the maximum turbulent shear stress of the gas phase located in the middle region of the boundary layer. The peak value increases and its location moves farther from the wall as the angle, θ, increases. The turbulent shear stress of the particle phase is generally lower than that of the fluid. While its maximum location remains unchanged when laden with particles, the turbulent shear stress of the gas phase for both the particle-laden flow cases is slightly lower than their counterpart in the single-phase flow. Similarly, it is also noticed that under the same particle loading ratio, the larger particles ($d_p = 120$ μm) seem to have greater effects on the fluid turbulence intensity, both the velocity fluctuations (figures 5 and 6) and the shear stress (figure 7) than the smaller particles ($d_p = 40$ μm).

4. DISCUSSION

4.1. *Particle response to mean velocity of the gas phase*

The gas velocity reduces greatly in the near wall region due to the high wall viscosity effect. This viscosity, together with the adverse pressure gradient along the tube wall surface, further results in a flow reversal near the wall, i.e. the separation of the boundary layer. Particles, whose inertia tends to make them maintain their initial velocities, however, decrease their velocities much more slowly than the gas. As a result, the particle phase shows higher velocities than the gas in the near wall region. Similarly, the larger particles flow even faster than the smaller ones near the wall. Physically, the particle's response to the mean fluid flow is most characterized by the particle's response time (Stokes time-constant, $\tau_p = \rho_p d_p^2/18\mu$), thus we find the smaller particles ($d_p = 40$ μm) with values of response time of 0.013 s flow with the mean fluid velocity generally more closely than the larger ones ($d_p = 120$ μm) whose response time is about 0.117 s.

4.2. *Modification of mean fluid velocity by particles*

The modification of mean fluid velocity by particles includes mainly two aspects. Firstly, the presence of the particles has resulted in greater fluid velocity gradients in the middle region of the boundary layer. Therefore the boundary layer becomes thinner for the particle-laden cross flow over the tube. This change is thought to arise from the momentum transfer between the gas phase and the particle phase. Notice that in the near region of the wall, because of the particles' inertia, the particulate phase velocity is higher than the gas phase velocity. The relative velocity between both phases obviously exists. Comparing mean gas phase velocity decays between single-phase and particle-laden flow cases in the near wall region, it can be found that the gas phase velocity of the particle-laden flow cases decays more slowly than the single-phase flow. The presence of the particle and the particle inertia augments the momentum sources of the gas phase, thus reducing the decay rate of the gas phase velocity. In a word, particles lag behind the gas phase and obtain momentum from the latter in the outer region of the boundary layer; as a result the mean velocities of the gas phase are reduced and show lower values than those in the single-phase flow. As a comparison, the momentum transfer occurs in the opposite

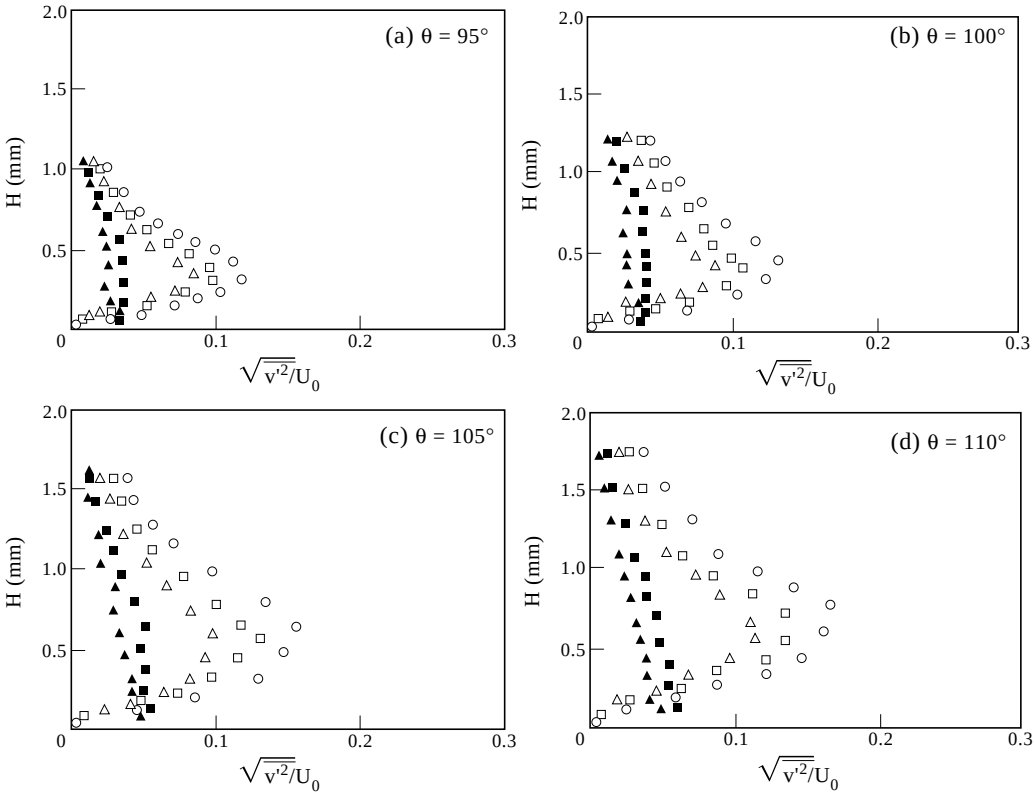

Figure 6. Radial r.m.s. velocity profiles in the boundary layer (○, single-phase flow; □, two-phase flow, $d_p = 40\ \mu$m; △, two-phase flow, $d_p = 120\ \mu$m; open symbols, gas phase; closed symbols, particles). (a) 95°; (b) 100°; (c) 105°; (d) 110°.

direction in the middle and near wall region since particles have higher velocities than the gas phase, thus increases in mean gas velocity can be expected in the particle-laden flow.

Secondly, the presence of particles has resulted in a definite delay in the boundary layer separation. Similarly, the above mentioned momentum transfer from the particles to the gas phase in the near region of the wall has attributed to this delay. Because particles take time to respond to the gas flow reversal, it can be found from figure 3 that, compared with the single-phase flow, the flow reversal of the particle-laden flow occurs with lower values of the reversal velocities and a small size of the flow reversal region. Besides, the particle/wall interaction may enhance the momentum exchange between the air flow close to the wall and thus also act to delay the boundary layer separation.

4.3. *Particle and fluid turbulence interaction*

The particle and fluid turbulence interaction obtained in the present experiments has many similarities to that documented by Tsuji *et al.* (1984) for an air–solid two-phase flow in a vertical pipe. The experimental results by Tsuji *et al.* (1984) showed the same trend of larger turbulence level attenuation by the particles in the end of the log region and the beginning of the wake region of the boundary layer. This uneven attenuation is most likely a result of the uneven drag loading, variations in the particle initial conditions, and particle/wall interactions. Moreover, Rashidi *et al.* (1990) found that the particles of 1100 μm diameter caused an increase in the turbulence level, while the particles of 120 μm diameter caused a decrease in the turbulence level. According to Hetsroni (1989), the fluid turbulence augmentation or attenuation can be accessed in terms of the particle Reynolds number ($\mathrm{Re}_p = |U_G - U_p| d_p/\nu$, where U_G and U_p are the gas phase velocity and the particle phase velocity). Turbulence enhancement is mostly associated with the wake effect or the vortex shedding downstream large particles. Achenbach (1974) has shown that vortex shedding occurs as $\mathrm{Re}_p > 400$. In the present study, we have Re_p ranges

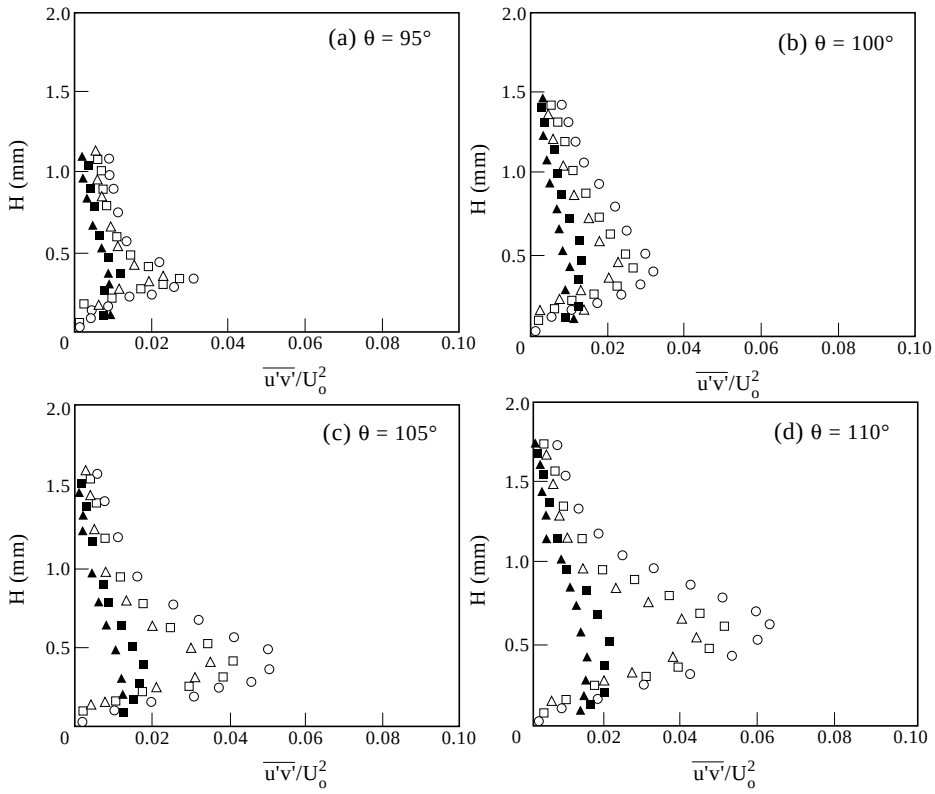

Figure 7. Reynolds shear stress profiles in the boundary layer (○, single-phase flow; □, two-phase flow, $d_p = 40\ \mu$m; △, two-phase flow, $d_p = 120\ \mu$m; open symbols, gas phase; closed symbols, particles). (a) 95°; (b) 100°; (c) 105°; (d) 110°.

of 20–32 for the smaller particles and 65–100 for the larger ones. For such values of Re_p ($Re_p < 100$), there is no vortex shedding to enhance the turbulence. On the contrary, particles have diffusion and dissipation effects on the turbulence energy when interacting with the turbulent eddies and thus attenuating the turbulence. It is also noticed that at the specified particle mass loading, the larger particles ($d_p = 120\ \mu$m) appear to have greater effects on the fluid turbulence intensity, both the velocity fluctuations and the shear stress, than the smaller particles. In addition, the examination of the shear stress profiles (figure 7) together with the mean velocity profiles (figure 3) shows that, just like other kinds of shear flow, the turbulent energy production term $-\overline{u'v'}(\partial U/\partial y)$ is most prominent in the strongest shear layer.

5. CONCLUSION

PDA measurements have been conducted to investigate the influence of the presence of the particles on the boundary layer characteristics for the cross flow over a tube. The results from the present experiment come to the following conclusions.

1. The mean fluid velocity profiles in the boundary layer are modified by the presence of the particles. The presence of the particles reduces the fluid flow reversal, delays the boundary layer separation point and results in a thinner boundary than that of the single-phase flow.
2. For the particle-laden flows, the attenuation of the r.m.s. velocity of the gas phase is observed at all measurement locations. This has been attributed to reductions in the fluid turbulence intensity and free shear layer fluctuations. These changes are most significant for the larger particles. Similar effects are also observed for the smaller particles, but little changes are noted.

Acknowledgements—The authors would like to acknowledge the financial support for this research provided by the National Natural Science Foundation of the People's Republic of China.

REFERENCES

Achenbach, E. (1974) Vortex shedding from spheres. *J. Fluid Mech.* **62,** 209–221.

Fitzpatrick, J. A., Lambert, B. and Murray, D. B. (1992) Measurements in the separation region of a gas–particle cross flow. *Expt. Fluids* **12,** 329–341.

Gore, R. A. and Crowe, C. T. (1989) Effect of particle size on modulating turbulence intensity. *Int. J. Multiphase Flow* **15,** 279–285.

Grass, A. J. (1974) Transport of fine sand on a flat bed: turbulence and suspension mechanics. In *Proc. Euromech.*, Tech. Univ. Denmark, Copenhagen, Vol. 48, p. 33.

Hetsroni, G. (1989) Particles–turbulence interaction. *Int. J. Multiphase Flow* **15,** 735–746.

Howarth, L. (1936) On the calculation of the velocity and temperature distributions for flow along a flat plate. *Proc. Roy. Soc.* **A154,** 364.

Inoue, A., Kozawa, Y., Yokosawa, M. and Aoki, S. (1986) Studies on two-phase cross flow. Part I: Flow characteristics around a cylinder. *Int. J. Multiphase Flow* **12,** 149–167.

Joo, Y. and Dhir, V. K. (1994) An experimental study of drag on a single tube and on a tube in an array under two-phase cross flow. *Int. J. Multiphase Flow* **20,** 1009–1019.

Lee, S. L. and Durst, F. (1982) On the motion of particles in turbulent duct flows. *Int. J. Multiphase Flow* **8,** 125–146.

Marble, F. E. (1963) *Combustion and Propulsion*. 5th AGRDograph Colloquium, Pergamon Press, p. 175.

Murray, D. B. (1989) The effect of solid particles on cross flow heat transfer. Ph.D. Thesis, University of Dublin, Ireland.

Murray, D. B. and Fitzpatrick, J. A. (1991) Heat transfer in a staggered tube array for a gas–solid suspension flow. *J. Heat Transfer* **113,** 865–873.

Rashidi, M., Hetsroni, G. and Banerjee, S. (1990) Particle–turbulence interaction in a boundary layer. *Int. J. Multiphase Flow* **16,** 935–949.

Rogers, C. B. and Eaton, J. K. (1991) The effect of small particles on fluid turbulence in a flat-plate, turbulent boundary layer in air. *Phys. Fluids* **A3,** 928–937.

Singleton, R. E. (1965) The compressible gas–solid particle flow over a semi-infinite flat plate. *ZAMP* **16,** 421.

Soo, S. L. (1965) Gas–solid flow. In *Proc. Symposium on Single and Multi-Component Flow Processes*, Engineering Research Publication No. 45, eds R. L. Peskin and C. F. Chen. Rutgers, New Brunswick, NJ, p. 1.

Soo, S. L. (1966) Fluid dynamics of multiphase system. AIChE Conference Paper No. 36E, Dallas, TX.

Sumer, B. M. and Deigaard, R. (1981) Particle motions near the bottom in turbulent flow in an open channel: Part 2. *J. Fluid Mech.* **109,** 311–337.

Tsuji, Y., Morikawa, Y. and Shiomi, H. (1984) LDV measurements of an air–solid two-phase flow in a vertical pipe. *J. Fluid Mech.* **139,** 417–434.

Yokosawa, M., Kozawa, Y., Inoue, A. and Aoki, S. (1986) Studies on two-phase cross flow. Part 2: Transition Reynolds number and drag coefficient. *Int. J. Multiphase Flow* **12,** 169–184.